ISSN 1674-1056
http://cpb.iphy.ac.cn
http://iopscience.iop.org/cpb
中国物理 B
Chinese Physics
中国物理
Chinese Physics B

Density functional theory analysis of electronic structure and optical properties of La doped Cd_2SnO_4transparent conducting oxide

Mei Tang(汤梅), JiaXiang Shang(尚家香), Yue Zhang(张跃)
Citation: Chin. Phys. B . 2018, 27(1): 017101. **doi:** 10.1088/1674-1056/27/1/017101

Journal homepage: http://cpb.iphy.ac.cn; http://iopscience.iop.org/cpb

What follows is a list of articles you may be interested in

Structural, electronic, and mechanical properties of cubic TiO_2:A first-principles study

Debashish Dash, Chandan K Pandey, Saurabh Chaudhury, Susanta K Tripathy
Chin. Phys. B . 2018, 27(1): 017102. **doi:** 10.1088/1674-1056/27/1/017102

Tuning electronic properties of the S_2/graphene heterojunction by strains from density functional theory

Jun-Hui Lei(雷军辉), Xiu-Fen Wang(王秀峰), Jian-Guo Lin(林建国)
Chin. Phys. B . 2017, 26(12): 127101. **doi:** 10.1088/1674-1056/26/12/127101

First-principle study of the structural, electronic, and optical properties of SiC nanowires

Wei-Hu Zhang(张威虎), Fu-Chun Zhang(张富春), Wei-Bin Zhang(张伟斌), Shao-Lin Zhang(张绍林), Woochul Yang
Chin. Phys. B . 2017, 26(5): 057103. **doi:** 10.1088/1674-1056/26/5/057103

Strain-induced magnetism in ReS_2 monolayer with defects

Xiao-Ou Zhang(张小欧), Qing-Fang Li(李庆芳)
Chin. Phys. B . 2016, 25(11): 117103. **doi:** 10.1088/1674-1056/25/11/117103

Theoretical optoelectronic analysis of intermediate-band photovoltaic material based on $ZnY_{1-x}O_x$(Y=S, Se, Te) semiconductors by first-principles calculations

Wu Kong-Ping, Gu Shu-Lin, Ye Jian-Dong, Tang Kun, Zhu Shun-Ming, Zhou Meng-Ran, Huang You-Rui, Zhang Rong, Zheng You-Dou
Chin. Phys. B . 2013, 22(10): 107103. **doi:** 10.1088/1674-1056/22/10/107103

Density functional theory analysis of electronic structure and optical properties of La doped Cd_2SnO_4 transparent conducting oxide

Mei Tang(汤梅)[1,2], JiaXiang Shang(尚家香)[1], and Yue Zhang(张跃)[1,†]

[1] *School of Materials Science & Engineering, Beihang University, Beijing* 100191, *China*
[2] *Journal Publishing Center of Tsinghua University Press, Beijing* 100084, *China*

(Received 23 August 2017; revised manuscript received 18 October 2017; published online 17 November 2017)

The electronic structural, effective masses of carriers, and optical properties of pure and La-doped Cd_2SnO_4 are calculated by using the first-principles method based on the density functional theory. Using the GGA+U method, we show that Cd_2SnO_4 is a direct band-gap semiconductor with a band gap of 2.216 eV, the band gap decreases to 2.02 eV and the Fermi energy level moves to the conduction band after La doping. The density of states of Cd_2SnO_4 shows that the bottom of the conduction band is composed of Cd 5s, Sn 5s, and Sn 5p orbits, the top of the valence band is composed of Cd 4d and O 2p, and the La 5d orbital is hybridized with the O 2p orbital, which plays a key role at the conduction band bottom after La doping. The effective masses at the conduction band bottom of pure and La-doped Cd_2SnO_4 are $0.18m_0$ and $0.092m_0$, respectively, which indicates that the electrical conductivity of Cd_2SnO_4 after La doping is improved. The calculated optical properties show that the optical transmittance of La-doped Cd_2SnO_4 is 92%, the optical absorption edge is slightly blue shifted, and the optical band gap is increased to 3.263 eV. All the results indicate that the conductivity and optical transmittance of Cd_2SnO_4 can be improved by doping La.

Keywords: transparent conducting oxides, electronic band structure, first-principle calculations, optical properties

PACS: 71.15.Mb, 71.20.–b, 78.20.–e, 42.50.Gy **DOI:** 10.1088/1674-1056/27/1/017101

1. Introduction

Since the 1980s, rapid progress was made in thin film technology, with fruitful achievements in both academic research and practical applications. The thin film technology and thin film materials have currently become one of the most focused research fields in material science. The transparent conductive thin film has drawn wide attention because of its high conductivity, high optical transmittance in the visible light range, and high reflectivity in the infrared light range. The transparent conductive thin film with the combination of transparency and conductivity has become a type of thin film characteristic of functional materials, and it has extensive application prospects in the optoelectronic industry.

After Badeker[1] sputtered cadmium for thermal oxidation for the first time to produce a transparent conductive cadmium oxide film in 1907, SnO_2-based thin films, In_2O_3-based thin films, and other different types of transparent conductive films[2] were successfully prepared and applied in many areas, forming a market of a certain size. Transparent conductive oxides (TCOs) are widely used in light-emitting diodes (LEDs), solar cells, flat panel displays (FDPs), and intelligent windows due to their excellent electrical and optical properties.[3] At present, the most widely used commercial material is indium tin oxide (ITO), which has high electrical conductivity, low optical absorption, and environmental stability.[4] However, due to the scarcity of indium resources and the high price, researchers are compelled to find and develop high-performance low-cost materials. When applied to solar cells, the sub-optimal conductivity and chemical/interfacial instability of ITO may cause problems and difficulties in meeting the future demand,[5] which have driven the search for alternative materials.

The next generation of photovoltaic cells will require thinner electrodes to simplify processing and improve performance. TCOs with higher conductivity are needed to keep the sheet resistance from decreasing when the thickness of the electrode reduces. The conductivity of TCOs can be enhanced by increasing the carrier density via chemical doping or reduction; however, increasing the carrier density will gear up the absorption by free carriers. Therefore, in order to obtain increased conductivity and high transparency, the mobility of TCOs must be promoted in the future. Recently, very high mobilities have been observed in a number of Cd-containing TCOs, including Cd_2SnO_4 (CTO) and $CdIn_2O_4$. The Cd_2SnO_4 transparent conductive film has the advantages of wide band gap, low resistivity, high visible light transmittance, and high carrier mobility, with a film resistivity of up to 10^{-6} Ω·cm and a mobility of up to 600 $cm^2/V{\cdot}s$.[6] In the visible range, the average transmittance is more than 90%.[7] Compared with SnO_2 thin films, Cd_2SnO_4 thin films have higher abrasive resistance and corrosion resistance, lower surface roughness, and are particularly stable. Compared with

†Corresponding author. E-mail: zhangy@buaa.edu.cn

© 2018 Chinese Physical Society and IOP Publishing Ltd

the ITO film, the Cd_2SnO_4 film is cheaper and can reduce the cost of solar thin film batteries. Cd_2SnO_4 thin films can also be widely used in transparent electrodes and various sensitive devices, displaying obvious advantages especially in the application of CdS, CdTe, and CIGS thin film solar devices. It has been found that the use of Cd_2SnO_4 transparent conductive thin film instead of a SnO_2 thin film layer can improve the thin film solar panel stability and cost performance. In recent years, many techniques have been adopted for the synthesis of Cd_2SnO_4 materials, such as sputtering, spray pyrolysis, the sol–gel method, co-precipitation, the thermal combustion method, and the hydrothermal method.[8–10] Although the basic transport mechanisms of the carriers in the CTO films and some of the physical properties of the films have been investigated for more than 3 decades, till now, there has not yet been a clear conclusion about the carrier mobility in CTO and only a limited number of first-principles calculations based theoretical studies have been reported. Ion doping is a method to improve the optical absorption characteristics of materials by introducing different impurity ions, controlling the micro crystal structure, and changing the band structure. The rare earth elements have many special photoelectric properties because of their incomplete occupied 4f electron orbits and empty 5d electron orbits, rich in electronic energy levels and long-lived excited states. They have become one of the new hotspots in the study of wide band gap semiconductor doping systems. Till now, there have been no reports on La-doped Cd_2SnO_4 in experiments. Thus, this paper aims to systematically investigate the effect of La doping on the electronic and optical properties of Cd_2SnO_4 on the basis of the first-principles calculations, which is helpful to direct the experimental study. In this paper, the electronic structural and optical properties of the orthorhombic Cd_2SnO_4 and La-doped Cd_2SnO_4 are studied. The band structure, total and partial density of states (TDOS and PDOS), effective masses of carriers, and optical properties of the La-doped Cd_2SnO_4 are calculated utilizing the first-principles method. An in-depth knowledge of the electronic structures and optical properties may theoretically shed some light on the modification of them.

2. Methods for calculation

Density functional theory (DFT), as a commonly used quantum mechanics method, is widely used to study the electronic structure of the multi-electron system in physics and chemistry. It has a wide range of physical and chemical applications and is one of the most commonly used methods for probing the electrical, mechanical, optical, and other properties of materials.[11–13] In this work, the calculations are performed by using the projector augmented wave (PAW) pseudopotentials based on the density functional theory (DFT), implemented in the Vienna *ab-initio* simulation package (VASP).[14–17] First, the cell structure is optimized so that the lattice constant is closest to the experimental value, and the reliability of the calculation method and the accuracy of the result are verified. Then, the optimized structure is subjected to atomic relaxation and static self-consistent calculation, the energy structure, density of states, effective mass, and optical properties of the system are calculated. The exchange and correlation potential is described by using the generalized gradient approximation (GGA), using the gradient function to modify the pseudopotential function and the projector augmented wave (PAW) pseudopotential to describe the interaction between the ions and electrons. The GGA+U method is carried out on a $2\times2\times1$ supercell of Cd_2SnO_4 containing 56 atoms. Hubbard U values are used for the O 2p states, Cd 3d states, and Sn 4d states in the electronic structure and optical property calculations. The cutoff energy is 500 eV and the Monkhorst–Pack k-point sampling is $10\times6\times3$ for the conventional cell of Cd_2SnO_4. The maximum stress and displacement are 0.01 GPa and 1×10^{-6} Å, respectively. The convergence criterion for self-consistent iteration is 10^{-5} eV/atom, and the other parameters are set to default.

3. Results and discussion

3.1. Structural properties

Cd_2SnO_4 possesses a space group of *Pbam* (No. 55) and an orthorhombic structure, in which tetrahedra and octahedra are stacked along the $\langle111\rangle$ direction. The tetrahedra and octahedra are occupied by Cd and Sn, respectively.[18] The lattice parameters of Cd_2SnO_4 are as follows: $\alpha=\beta=\gamma=90^\circ$, $a=3.24937$, $b=5.66477$, $c=10.12710$. The supercell technology is employed to model the La-doped Cd_2SnO_4, where a $2\times2\times1$ supercell is built up. In our calculations, the structure of La-doped Cd_2SnO_4 is modeled by replacing one Cd atom in the surpercell with one La atom. The $Cd_{1.9375}La_{0.0625}SnO_4$ supercell model is displayed in Fig. 1. The supercell is structurally optimized until the force on all atoms is less than 0.01 eV/Å, and then the resulting optimized structure is used for the subsequent electronic structure and optical properties calculations.

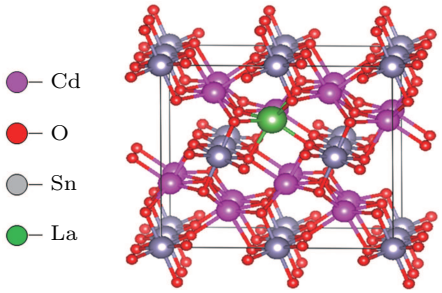


Fig. 1. (color online) Super cell ($2\times2\times1$) of La-doped Cd_2SnO_4.

3.2. Band structures and density of states

In this research, we employ the GGA+U method to calculate the structural and optical properties of the pure and La-doped Cd_2SnO_4. By using the GGA functional defined by Perdew–Burke–Ernzerhof (GGA-PBE), the calculated band gap of pure Cd_2SnO_4 is 0.416 eV, which is in good agreement with the data from other DFT based calculations, and the band structure is shown in Fig. 2(a). The calculated band structure shows that the valence band maximum (VBM) and the conduction band minimum (CBM) are located at the Γ point of the Brillouin zone, which indicates that Cd_2SnO_4 is a direct band-gap semiconductor. The calculated band gap is much smaller than the experimental value due to the well known Kohn–Sham error in DFT calculations when d and f orbitals are involved.[14] To correct this error, the GGA+U method is employed to improve the band gap value by up to 2.216 eV, which is in good agreement with experimental data, as shown in Fig. 2(b). The U parameters of the O, Cd, Sn atoms are 8 eV, 10 eV, and 9 eV, respectively, which are adjusted to reach an agreement with the experimental band gap of Cd_2SnO_4 ($E_g = 2.3$–2.5 eV).[18,19] The same parameters are used for the La-doped Cd_2SnO_4. The band structure is shown in Fig. 2(c). It can be seen from Fig. 2(c) that the Fermi level shifts upward into the conduction band after the La atom is doped in Cd_2SnO_4, which produces a degenerate n-type semiconductor, and the band gap is decreased to 2.02 eV. Due to the Burstein–Mott effect, the optical band gap is increased to 3.263 eV,[19] which is measured between the Fermi level in the conduction band and the valence band maximum (VBM). The reason for the changes in the band structure may be that the ionic radius of La^{3+} (0.106 nm) is larger than that of Cd^{2+} (0.084 nm), but the electronegativity of La (1.11) is smaller than that of Cd (1.69). When La is doped, due to the changes of the atomic structure and electronegativity, the doped system changes in both space and charge distribution. The valence electron structure of La is $5d^16s^2$, after the substitution of Cd atom, an electron is added to form a localized positive center, and an electron capture center is formed to capture electrons.[20] Therefore, the impurity energy level is introduced at the bottom of the conduction band, that is, the 5d orbital of the La atom is hybridized with the O 2p orbital, leading to the broadening of the conduction band and the conduction band moving towards low energy levels, thus decreasing the band gap.

The total and partial densities of states of pure and La-doped Cd_2SnO_4 are presented in Fig. 3. The DOS in Fig. 3(a) illustrates the composition of the conduction band and the valence band. The conduction band is mainly composed of Cd 5s, Sn 5s, and Sn 5p orbits, and the overlapping of Cd 4d with O 2p makes up the valence band top. When the La atom is doped in Cd_2SnO_4, the La 5d orbit occupies the bottom of the conduction band around the Fermi level (see Fig. 3(b)). These donor states of the Fermi energy level provide n-type carriers which enhance the conductivity of Cd_2SnO_4 and thus affect the optical properties.

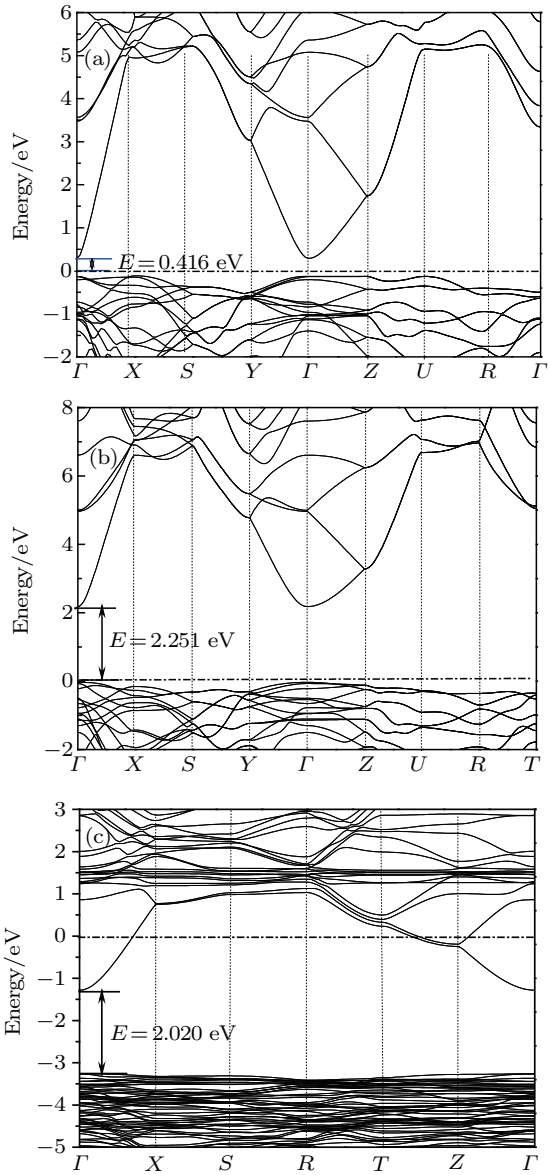


Fig. 2. (a) The band structure of the Cd_2SnO_4 based on PBE; (b) the band structure of the Cd_2SnO_4 based on GGA+U; (c) the band structure of the La doped Cd_2SnO_4 based on GGA+U.

It is noteworthy that the DOS of the conduction band in Fig. 3(a) varies dramatically with the variation of k. The velocity of the electron in the k-space is proportional to the slope of the DOS, so in the conduction band of Cd_2SnO_4 the photo excited electrons possess a large velocity, which can help separate and transfer the photo-excited carriers to the surface of Cd_2SnO_4. This might explain why Cd_2SnO_4 possesses high O_2 evolution activities under the visible-light irradiation.[21]

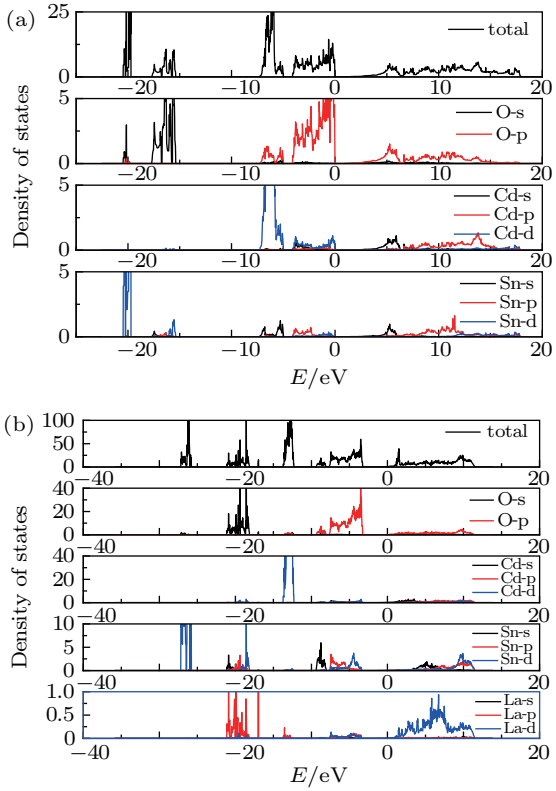


Fig. 3. (color online) DOS and PDOS of (a) pure Cd_2SnO_4 and (b) La-doped Cd_2SnO_4.

3.3. Effective mass of carriers

For CTO materials, the conductivity is a very important parameter. The conductivity of the material is proportional to the carrier mobility. The carrier mobility mainly depends on the average free time and the effective mass of the carrier as

$$\mu = q\tau/m^*, \tag{1}$$

where μ is the carrier mobility, q is the amount of charge carried by the carrier, τ is the average free time of the carrier, and m^* is the effective mass of the carrier. τ is the time between continuous scattering of the carriers during the drift motion under the action of the electric field, so it depends mainly on the material defects, scattering mechanisms, the environment such as temperature, and other external factors. Therefore, the effective mass of the carrier will play an intrinsic and essential role in the electrical conductivity of the material, and so it is of great significance to study the effective mass of the carriers.

According to the definition of the effective mass, it can be calculated by

$$\frac{1}{m^*} = \frac{1}{h}\frac{\mathrm{d}^2E(k)}{\mathrm{d}k^2}, \tag{2}$$

where $\hbar$ is the Planck constant, and $\mathrm{d}^2E(k)/\mathrm{d}k^2$ is the second derivative of energy $E(k)$ with respect to wave vector k. The effective mass at the bottom of the conduction band and the top of the valence band can be calculated by fitting the bottom of the conduction band and the top of the valence band. By fitting the conduction band in the band diagram (see Fig. 2), we can obtain the second derivative $\mathrm{d}^2E(k)/\mathrm{d}k^2$.

The relationship between the curvature of the band and the effective mass of the excitons is given by[22]

$$m^* = m_0/2c, \tag{3}$$

where c is the coefficient of the second-order term in a quadratic fit of $E(k)$. Here, a larger coefficient of the second-order term corresponds to a lower effective mass of the charge carrier, indicating a higher mobility of the charge carrier.

It can be seen from Fig. 2 that the valence band for pure Cd_2SnO_4 and La-doped Cd_2SnO_4 is flatter than the conduction band, indicating that the valence band holes are heavier than the conduction band electrons. Therefore, we only calculate the curvature of the parabolic portions of the band near the conduction band minimum (CBM) to describe the transport phenomena in the semiconductors.

The m^* of CBM for pure Cd_2SnO_4 and La-doped Cd_2SnO_4 are $0.18m_0$ and $0.092m_0$, respectively, which are in good conformity with the experimental data (0.2–$0.5m_0$).[4] Compared with pure Cd_2SnO_4, La-doped Cd_2SnO_4 exhibits a lower effective mass of the electrons in the conduction band, indicating that the conductivity of Cd_2SnO_4 can be improved by doping La.

3.4. Optical properties

Optical properties are another important property of CTO materials, depending on the transition of electrons between different levels. The optical performance is very sensitive to the changes in the electronic structure. The absorption and emission of light by a solid material are mainly caused by the interaction of photons with electrons, atoms, or ions in the material. The dielectric function can be obtained by the first-principles calculation to study the optical properties of materials. The dielectric function is $\varepsilon(\omega) = \varepsilon_1(\omega) + \mathrm{i}\varepsilon_2(\omega)$.[22,23] The real part $\varepsilon_1(\omega)$ represents the dispersion of the incident photons by the material and can be evaluated from the Kramer–Kronig relationship, while the imaginary part of the dielectric function $\varepsilon_2(\omega)$ is directly related to the light absorption coefficient, which can directly reflect the actual transition between the occupied state below the Fermi level and the unoccupied state above the Fermi level. The real and imaginary parts of the dielectric function can be derived from the VASP program output file, and other common optical constants, such as absorption coefficient, reflectivity, and transmittance can be derived from $\varepsilon_1(\omega)$ and $\varepsilon_2(\omega)$.[24–31]

The imaginary part of the dielectric function $\varepsilon_2(\omega)$ of pure and La-doped Cd_2SnO_4 is calculated, which is presented in Fig. 4. Considering the tensor nature of the dielectric function, the imaginary parts of the dielectric function are averaged over three polarization vectors (x, y, and z) in our

calculations. From Fig. 4, as for La-doped Cd_2SnO_4, the trend is similar with pure Cd_2SnO_4. A new peak is found in the low energy around 0.40 eV for the La-doped Cd_2SnO_4, which originates from the excitation of O 2p electron from the top of the valence band to the impurity energy level located at the bottom of the conduction band.

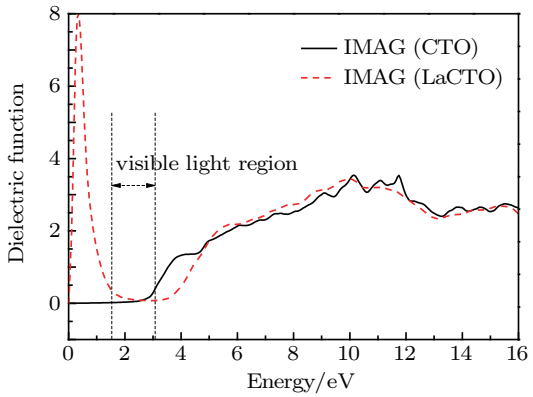


Fig. 4. (color online) The imaginary part of the dielectric function of pure and La-doped Cd_2SnO_4.

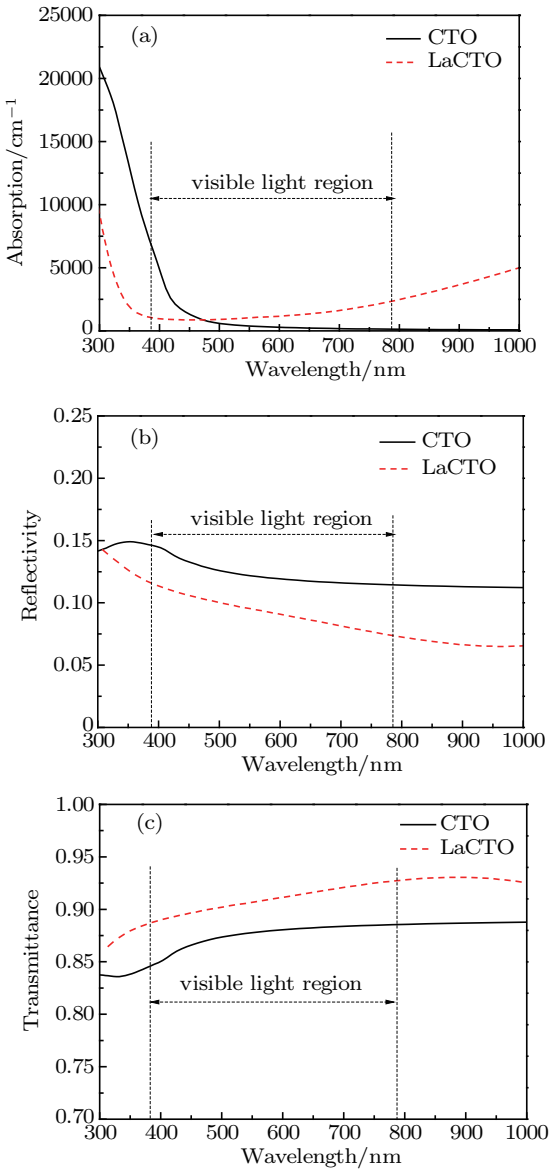


Fig. 5. (color online) (a) Absorption, (b) reflectivity, and (c) transmittance of pure and La-doped Cd_2SnO_4.

As shown in Fig. 5(a), the absorption edge of pure Cd_2SnO_4 in the visible region is about 480 nm, which is in conformity with experimental results (about 500 nm),[18] while the absorption edge is about 380 nm for La-doped Cd_2SnO_4. When Cd_2SnO_4 is doped by La, the occupied states close to the bottom of the conduction band are mainly shallow donor states, whereby the absorption is obvious in the infrared region but relatively low in the visible region. In addition, the absorption band edge is blue shifted, this is mainly due to the so-called Burstein–Moss effect. In Fig. 5(b), it is obvious that pure Cd_2SnO_4 has a reflectivity of 12% in the visible and infrared regions. However, the reflectivity of La-doped Cd_2SnO_4 in the visible and infrared regions is significantly reduced to less than 10%, the change of the reflectivity constant provides a theoretical basis for the development of new dielectric materials and reflective materials. Figure 5(c) shows the transmission spectra of pure and La-doped Cd_2SnO_4. It can be seen from the figure that the average transmittance is around 88% for pure Cd_2SnO_4 and 92% for La-doped Cd_2SnO_4, demonstrating that the optical transmittance of Cd_2SnO_4 can be improved by doping La.

4. Conclusion

The electronic structure and optical properties of pure and La-doped Cd_2SnO_4 have been investigated in this research using the GGA+U method based on the first-principles calculations. It is found that the calculated band gap of Cd_2SnO_4 is close to the experimental data and the conductivity of Cd_2SnO_4 can be improved by doping La, which is in good conformity with other theoretical calculations. After La doping, the band gap slightly decreases but the optical band gap increases, which leads to a blue shift, with the transmittance of the visible regions being improved. Moreover, in the vicinity of the Fermi level at the bottom of the conduction band, the hybridization of the La 5d orbit and O 2p orbit creates shallow donor states. Adjustment of the band structure via overlapping of Cd 4d with O 2p could be anther feasible way of developing and designing oxide photocatalysts working in the visible light. These salient features make La doped Cd_2SnO_4 an ideal transparent conductive oxide for optoelectronic device applications.

References

[1] Badeker K 1907 *Ann. Phys.* **22** 749
[2] Chopra K L, Major S and Pandya D K 1983 *Thin Solid Films* **102** 1
[3] Niu M, Cheng D J, Huo L J and Shao X H 2012 *J. Alloys Compd.* **539** 221
[4] Jeyadheepan K, Thamilselvan M, Kim K and Sanjeeviraja C 2015 *J. Alloys Compd.* **620** 185

[5] Al-Baradi A M, El-Nahass M M, El-Raheem M M A, Atta A A and Hassanien A M 2014 *Radiat. Phys. Chem.* **103** 227
[6] Kammler D R, Mason T O and Poeppelmeier K R 2000 *Chem. Mater.* **121** 954
[7] Xu J, Huang S P and Wang Z S 2009 *Solid State Commun.* **149** 527
[8] Krishnakumar V, Ramamurthi K, Kumaravel R and Santhakumar K 2009 *Curr. Appl. Phys.* **9** 467
[9] Godines C D, Castanedo C T, Pérez R C, Delgado G T and Ángel O Z 2014 *Sol. Energy Mater. Sol. Cells* **128** 150
[10] Sidorak A V, Ivanov V V and Shubin A A 2011 *Mater. Sci. Appl.* **2** 1219
[11] Zhou W, Liu L J, Yuan M Y, Song Q G and Wu P 2012 *Comput. Mater. Sci.* **54** 109
[12] Rezkallah T, Chemam F and Djabri I 2017 *Chin. Phys. B* **26** 027102
[13] Wang S, Du Y L and Liao W H 2017 *Chin. Phys. B* **26** 017806
[14] Farooq R, Mahmood T and Anwar A W 2016 *Superlattice. Microst.* **90** 165
[15] Clark S J and Robertson J 2010 *Phys. Rev. B* **82** 085208
[16] Deng J J, Liu B, Gu M, Liu X L, Huang S M and Ni C 2012 *Acta Phys. Sin.* **61** 036105 (in Chinese)
[17] Du Y J, Chang B K, Zhang J J, Li B, and Wang X H 2012 *Acta. Phys. Sin.* **61** 067101 (in Chinese)
[18] Liu D, Ren S Q, Ma X, Liu C, Wu L L, Li W, Zhang J Q and Feng L H. 2017 *RSC Adv.* **7** 8295
[19] Dinesh S, Anandan M, Premkumar V K, Barathan S, Sivakumar G and Anandhan N 2016 *Mater. Sci. Eng. B* **214** 37
[20] Velusamy P, Ramesh Babu R, Ramamurthi K, Elangovan E and Viegas J 2017 *J. Alloy. Compd.* **708** 804
[21] Khatun M R, Hossain M M, Ali M A and Jahan N 2017 *Chin. Phys. B* **26** 033102
[22] Slassi A 2015 *Optik* **126** 4751
[23] Zhang X D, Guo M L and Liu C L 2008 *Appl. Phys. Lett.* **93** 012103
[24] Slassi A 2015 *Opt. Quant. Electron.* **47** 2465
[25] Wu H C, Peng Y C and Shen T P 2012 *Materials* **5** 2088
[26] Zhang Y J, Yan J L and Zhao G 2010 *Physica B* **405** 3899
[27] Zhang H J, Liu L and Zhou Z 2012 *Phys. Chem. Chem. Phys.* **14** 1286
[28] Li X N, Gessert T A and Coutts T 2004 *Appl. Surface Sci.* **223** 138
[29] Han J C, Gao W and Zhu J Q 2007 *Phys. Rev. B* **75** 101
[30] Du J J and Li W 2012 *Adv. Mater. Res.* **476–478** 1154
[31] Yoffe A D 2001 *Adv. Phys.* **50** 1